

## University of New Hampshire University of New Hampshire Scholars' Repository

---

Faculty Publications

---

12-1-1996

# Ground-based measurements of NO<sub>x</sub> and total reactive oxidized nitrogen (NO<sub>y</sub>) at Sable Island, Nova Scotia, during the NARE 1993 summer intensive

T. Wang

M. A. Carroll

G. M. Albercook

K. R. Owens

Katharine A. Duderstadt

*University of New Hampshire, Durham*, [katharine.duderstadt@unh.edu](mailto:katharine.duderstadt@unh.edu)

*See next page for additional authors*

Follow this and additional works at: [https://scholars.unh.edu/faculty\\_pubs](https://scholars.unh.edu/faculty_pubs)

---

### Recommended Citation

Wang, T., M.A. Carroll, G.M. Albercook, K.R. Owens, K.A. Duderstadt, A.N. Markevitch, D.D. Parrish, J.S. Holloway, F.C. Fehsenfeld, G. Forbes, J. Ogren (1996), Ground-based measurements of NO<sub>x</sub> and total reactive oxidized nitrogen NO<sub>y</sub> at Sable Island, Nova Scotia, during the NARE 1993 summer intensive, *J.Geophys. Res.*, 101, 28,991-29,004, doi:10.1029/96JD01090.

This Article is brought to you for free and open access by University of New Hampshire Scholars' Repository. It has been accepted for inclusion in Faculty Publications by an authorized administrator of University of New Hampshire Scholars' Repository. For more information, please contact [nicole.hentz@unh.edu](mailto:nicole.hentz@unh.edu).

---

**Authors**

T. Wang, M. A. Carroll, G. M. Albercook, K. R. Owens, Katharine A. Duderstadt, A. N. Markevitch, D. D. Parrish, J. S. Holloway, F. C. Fehsenfeld, G. Forbes, and J. Ogren

## Ground-based measurements of NO<sub>x</sub> and total reactive oxidized nitrogen (NO<sub>y</sub>) at Sable Island, Nova Scotia, during the NARE 1993 summer intensive

T. Wang<sup>1,2</sup>, M. A. Carroll<sup>1,3</sup>, G. M. Albercook<sup>1</sup>, K. R. Owens<sup>1,3</sup>, K. A. Duderstadt<sup>1</sup>, A. N. Markevitch<sup>1</sup>, D. D. Parrish<sup>4</sup>, J. S. Holloway<sup>4</sup>, F. C. Fehsenfeld<sup>4</sup>, G. Forbes<sup>5</sup>, and J. Ogren<sup>6</sup>

**Abstract.** Measurements of NO, NO<sub>2</sub>, and total reactive oxidized nitrogen (NO<sub>y</sub>) were added to ongoing measurements of aerosols, CO, and O<sub>3</sub> at Sable Island (43°55'N, 60°01'W), Nova Scotia, during the North Atlantic Regional Experiment (NARE) 1993 summer intensive. Ambient levels of NO<sub>x</sub> and NO<sub>y</sub> were found to be highly variable, and elevated levels can be attributed to the transport of polluted continental air or presumably to relatively fresh emissions from sources upwind (e.g., ship traffic). The median values for NO<sub>x</sub> and NO<sub>y</sub> are 98 and 266 parts per trillion by volume (pptv), respectively. A multiday pollution episode occurred during which elevated NO<sub>x</sub> and NO<sub>y</sub> were observed with enhanced levels of O<sub>3</sub>, CO, and condensation nuclei. Air masses of recent tropical marine origin characterized by low and constant levels of O<sub>3</sub> and CO were sampled after Hurricane Emily. The correlation between ozone and CO is reasonably good, although the relation is driven by the single pollution episode observed during the study. The correlation of O<sub>3</sub> with NO<sub>y</sub> and with NO<sub>y</sub>-NO<sub>x</sub> is complicated by the presumed NO<sub>y</sub> removal processes in the marine boundary layer. Examination of the radiosonde data and comparisons of the surface data with those obtained on the overflying aircraft provide clear indications of vertical stratification above the site.

### 1. Introduction

Active and reservoir reactive nitrogen compounds play an important role in tropospheric chemistry. Oxides of nitrogen (NO<sub>x</sub> = NO + NO<sub>2</sub>) are critical in determining atmospheric oxidation rates by influencing the photochemical production of ozone and, consequently, hydroxyl radical concentrations in the troposphere [e.g., Crutzen, 1974, 1979; Chamedies, 1978; Fishman et al., 1979; Fishman, 1985; Liu et al., 1980, 1983, 1987; Logan et al., 1981; Logan, 1983, 1985]. Recent studies indicate that background levels of O<sub>3</sub> in rural areas of both the northern and the southern hemispheres may have increased by as much as a factor of 2 during the past 100 years and that the tropospheric ozone budget is now strongly influenced by photochemical production resulting from increased levels of NO<sub>x</sub> [e.g., Volz and Kley, 1988; Sandroni et al.,

1992]. Additionally, evidence from satellite measurements indicates that O<sub>3</sub> exported from the source regions may contribute to the abundance of tropospheric O<sub>3</sub> in remote marine environments [e.g., Fishman et al., 1986, 1990; Fishman and Larsen, 1987; Parrish et al., 1993a; Jacob et al., 1993].

Measurements of total reactive oxidized nitrogen (NO<sub>y</sub>), especially in conjunction with measurements of speciated reactive nitrogen, have proven to be valuable in assessing the photochemical processing that has occurred in an air parcel [e.g., Fahey et al., 1986; Doddridge et al., 1991; Jaffe et al., 1991; Ridley, 1991; Parrish et al., 1991, 1993b; Atlas et al., 1992; Hübler et al., 1992; Sandholm et al., 1992, 1994]. In this paper, total reactive oxidized nitrogen is defined as NO<sub>y</sub> = NO + NO<sub>2</sub> + NO<sub>3</sub> + 2N<sub>2</sub>O<sub>5</sub> + HONO + HO<sub>2</sub>NO<sub>2</sub> + PAN + HNO<sub>3</sub> + aerosol nitrate + other organic nitrates (where N is in the ≥ +II oxidation state). Since the concentration of total reactive oxidized nitrogen is a more conserved quantity than the concentrations of the individual NO<sub>y</sub> species, the observed relationship among NO<sub>y</sub> and other tracers such as CO, C<sub>2</sub>Cl<sub>4</sub>, and O<sub>3</sub> can aid in testing our current understanding of the sources of these compounds [e.g., Hübler et al., 1992]. In addition, the distribution and chemistry of NO<sub>y</sub> is of primary interest in establishing inflow/outflow regional budgets for nitrogen with regard to the tropospheric acid transport/deposition problem [Fehsenfeld et al., 1987].

Emissions of ozone precursors along the eastern coast of North America can be transported to the temperate North Atlantic Ocean. A recent study by Parrish et al. [1993a] based on the measurements of CO and O<sub>3</sub> conducted at three island sites in the Canadian Maritime Provinces (including Sable Island, the site of this present study) shows that elevated O<sub>3</sub> is often correlated with high levels of CO in the summer months.

<sup>1</sup>Department of Atmospheric, Oceanic, and Space Sciences, University of Michigan, Ann Arbor.

<sup>2</sup>Now at Environmental Engineering Unit, Department of Civil and Structural Engineering, Hong Kong Polytechnic University, Hung Hom, Kowloon, Hong Kong.

<sup>3</sup>Also at Department of Chemistry, University of Michigan, Ann Arbor.

<sup>4</sup>Aeronomy Laboratory, National Oceanic and Atmospheric Administration, Boulder, Colorado.

<sup>5</sup>Atmospheric Environment Service, Sable Island, Nova Scotia, Canada.

<sup>6</sup>Climate Monitoring and Diagnostics Laboratory, National Oceanic and Atmospheric Administration, Boulder, Colorado.

Parrish *et al.* [1993a] concluded that the observed linear relationship between ozone and CO indicates summertime photochemical production of ozone from anthropogenic precursors emitted from the source region on the North American continent. In the summer of 1993 (July-September), the North Atlantic Regional Experiment (NARE) 1993 summer intensive was conducted to study the influence of anthropogenic emissions (mainly from the North American continent) on the distribution of ozone and its precursors over the North Atlantic. A detailed description of the NARE program and the summer intensive is presented by Fehsenfeld *et al.* [this issue, (a & b)]. During this campaign, measurements of NO, NO<sub>2</sub> and NO<sub>y</sub> (made by the University of Michigan) were added to ongoing measurements of O<sub>3</sub>, CO (D. D. Parrish and J. S. Holloway, NOAA Aeronomy Laboratory, 1993), and aerosol scattering coefficients, number concentration, and composition (J. Ogren, NOAA Climate Monitoring and Diagnostics Laboratory, 1993) at Sable Island, Nova Scotia. In addition, solar UV radiation and water vapor content were measured, and grab samples were collected in canisters and were later analyzed for nonmethane hydrocarbons (D. Blake and N. Blake, the University of California at Irvine, 1993). This paper focuses on the abundance and variability of reactive nitrogen compounds and their relationship with O<sub>3</sub> and CO.

## 2. Experiment

### 2.1. Site Description

The measurements were made at Sable Island (43°55'N; 60°01'W), Nova Scotia, Canada (see Figure 1). The island is located approximately 180 km off the coast of Nova Scotia and is about 300 km east of Halifax. Physically, the island is 40 km long and approximately 1 km wide. It is composed of small sand dunes (< 30 m in height) covered with grass and other low vegetation. It is a refuge for seals, wild horses, and migratory birds. Public access is restricted, and the only permanent residents are the staff of the Canadian Atmospheric Environment Service weather station. The measurement site was at the weather station which is approximately 8 km from the western end of the island, 100 m from the north beach, and 800 m from the south beach. Ongoing measurements of O<sub>3</sub> and CO were carried out in the main operation building (see Parrish *et al.*, [1993a] for details), whereas measurements of reactive nitrogen, aerosols, and wind speed and direction were made in a building located approximately 100 m southwest of the main operation building. A 10-m scaffold was erected next to the instrument building to mount the NO<sub>x</sub> and NO<sub>y</sub> inlet systems.

The only major source of pollution on the island was a set of diesel generators for the weather station located approximately 180 m to the east of the sampling site, downwind of prevailing southwesterly flow. Other island sources included the oil-fired water heaters of the residences located to the northeast and infrequent local vehicle traffic. An oil production platform is located approximately 40 km to the southwest of the island, and two ships are permanently stationed there. Ship traffic in the vicinity of the island is erratic. Depending on weather conditions, transatlantic shipping routes occasionally pass 20 to 40 km north and south of the island. Emissions from the oil production facility (flaring and power generation) as well as from ships may have influenced the observed levels of chemical species at Sable Island.

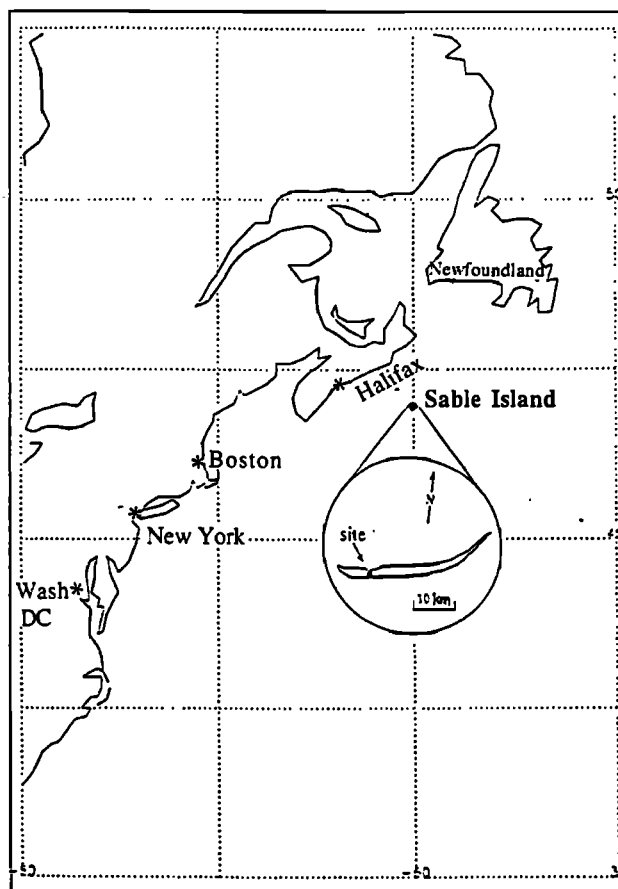


Figure 1. A map showing the relation of Sable Island with the eastern coast of North America.

### 2.2. Instrumental Methods

Nitric oxide was measured with a chemiluminescence detector utilizing the reaction of NO with O<sub>3</sub>, and ambient NO<sub>2</sub> was measured by photolyzing NO<sub>2</sub> to NO upstream with subsequent detection of NO [e.g., Ridley *et al.*, 1987, 1988, 1989; Carroll *et al.*, 1990a,b, 1992]. One detector alternated between measuring NO and NO<sub>2</sub>. NO<sub>y</sub> species were converted to NO on a gold catalyst with CO as a reducing reagent [Bollinger *et al.*, 1983; Fahey *et al.*, 1985, 1986], followed by chemiluminescence detection of NO using a second detector. Only the features relevant to this field study will be described in detail.

Figure 2 shows a schematic of NO<sub>x</sub> and NO<sub>y</sub> inlet systems. Ambient air was sampled at a height of approximately 9 m on a 10-m scaffold. For NO<sub>x</sub> detection, ambient air was sampled through the photolysis cell (Pyrex glass; ID, 6.4 cm; length, 38 cm) at a flow rate of 2 standard liters per minute (slpm). The residence time of sampled air in the sampling system (3/8 inch PFA sample line and photolysis cell) was less than 7 s (~ 5.7 s in the photolysis cell). The pressure within the cell was maintained at 125 torr and the temperature of the cell was maintained at ~ 13°C. Operation of the photolysis cell at reduced pressure was required due to the use of a large cell. By lowering the pressure, concentrations of ozone and water vapor in the sampled air were lowered, which prevented condensation and reduced interfering reactions between ambient ozone and NO within the photolytic cell. A 300 W, high-pressure, Xe arc lamp was used to photolyze NO<sub>2</sub> molecules. A

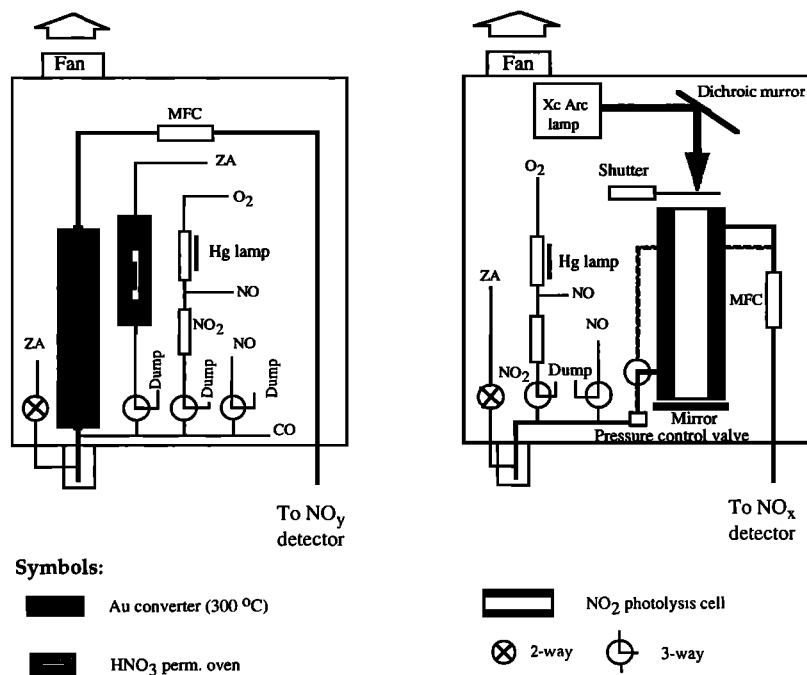


Figure 2. Schematic of the NO<sub>x</sub> and NO<sub>y</sub> inlets.

mechanical shutter controlled by a computer either blocked the light from the lamp (NO mode) or allowed it to pass through the cell (NO<sub>2</sub> mode).

For NO<sub>y</sub> measurements, ambient air was drawn at a rate of 1 slpm through a gold-plated stainless steel inlet provided by D. D. Parrish (ID, 0.19 inches; length, 3.5 inches; heated to 100°C) into the gold catalytic converter maintained at 300°C. Three standard cubic centimeters per minute (sccm) of carbon monoxide from an aluminum cylinder (99.99%, Scott Specialty Gases) was added to the sample stream. The gold-plated inlet was made as short as possible and heat was added to minimize the loss of HNO<sub>3</sub> in the inlet.

Since mass flowmeters can be sensitive to temperature changes, both of the mass flow controllers in the NO<sub>x</sub> and NO<sub>y</sub> inlet boxes were held at 35°C. To avoid any contamination of sampled air by the inlet boxes, both enclosures were equipped with a 6-inch fan, and exhaust was vented through a dryer hose extending 15 m away from the sampling platform. The two chemiluminescence detectors, along with the ozone sources, calibration module and data acquisition and control systems, were located inside the same building housing the instruments for measuring aerosols and the data acquisition system for recording wind speed and wind direction measurements. Pump exhaust and dumped calibration standards were also vented through the dryer hose.

Calibrations were conducted roughly every 3.5 hours by adding a small flow of standard gas to the ambient airstream. Calibration standards were added at levels of ~ 3 parts per billion by volume (ppbv). The NO standard mixture (in N<sub>2</sub>, Scott Marris Inc.) was compared with the National Institute of Standards and Technology (NIST) Standard Reference Material, and it agreed (difference < 3%). A flowing NO<sub>2</sub> standard was generated via titration of the NO standard with O<sub>3</sub> generated by photolyzing O<sub>2</sub> with a mercury vapor lamp. The NO<sub>2</sub> standard was used to determine the conversion efficiencies of both the photolytic and the catalytic converters. In addition, gaseous

HNO<sub>3</sub> obtained from a permeation tube was used to check the catalytic converter efficiency in the field and in the laboratory after the field experiment. Since the level of NO<sub>2</sub> (extent of titration) was found to vary with time, it was determined indirectly by quantifying the NO remaining after titration during each calibration period.

Throughout the experiment, the sensitivities of both detectors with respect to NO were very stable. Average instrument sensitivity was 4.87 (standard deviation, ±0.13) counts per second per parts per trillion by volume (cps/pptv) for the NO<sub>x</sub> detector and 3.80 (standard deviation, ±0.09) cps/pptv for the NO<sub>y</sub> detector. The efficiency of the NO<sub>2</sub> photolytic converter ranged from ~ 16% at the beginning of the experiment (as a result of imperfect optics adjustment) to ~ 24% throughout the rest of the experiment. The Xe lamp was not replaced during the experiment (23 days) since there was no indication of a decreasing NO<sub>2</sub> conversion efficiency. In the NO<sub>y</sub> detection system the NO<sub>2</sub> conversion efficiency in the gold converter never dropped below 95% (in both ambient air and synthetic air). During the field study, the HNO<sub>3</sub> conversion efficiency was evaluated in zero air (HNO<sub>3</sub> was added at the position of 2 inches from the front end of the sample inlet tube, Figure 2). However, the signal of the NO<sub>y</sub> detector was not stable and exhibited sinusoidal behavior for a 3-hour period, which may be attributed to unstable delivery of the HNO<sub>3</sub> standard. After the field study, a similar test was conducted in our laboratory on the two converters used in the field, without reconditioning following their most recent use in hopes of maintaining them in the same condition as in the field. The results show that the HNO<sub>3</sub> in zero air was converted at an efficiency of ~ 95% and ~ 100% on the two converters, respectively. The efficiency was determined by comparing the signal of the NO<sub>y</sub> detector when the Au catalyst was maintained at 300°C to that at 500°C, assuming that nitric acid was converted completely at 500°C. The high conversion efficiency of HNO<sub>3</sub> obtained in the lab was taken as an indication that HNO<sub>3</sub> was converted at

high efficiency in the field as well because (1) both converters were routinely reconditioned, as described below, every second day throughout the study period; and (2) field tests conducted by the NOAA Aeronomy Lab group at a similar North Atlantic site (Chebogue Point, Nova Scotia) showed that high conversion efficiency (> 84%) of HNO<sub>3</sub> in ambient air was achieved and maintained through a similar but even less frequent reconditioning practice. The designs of the converter and the inlet used by the UM group are identical to those used by AL group.

Artifact tests, cleaning of the photolysis cell, and reconditioning of the gold catalyst were typically carried out every other day. During artifact tests, ultrapure zero air (Scott Marrin Inc.) was used in place of ambient air. During the experiment, 23 such tests were conducted. Average artifact signals are  $1.3 \pm 1.0$  (standard deviation) pptv for NO and  $7.4 \pm 3.3$  pptv for NO<sub>2</sub>. The NO<sub>y</sub> system showed artifact signals that decreased with time, with a value of ~ 100 pptv observed at the beginning of the experiment dropping to ~ 20 pptv toward the end of the study, excepting a brief period when a signal as high as 200 pptv was observed immediately after the HNO<sub>3</sub> conversion efficiency test. The mean NO<sub>y</sub> artifact was 53 pptv with a standard deviation of 39 pptv. During data reduction, artifact signals in NO, NO<sub>2</sub>, and NO<sub>y</sub> modes were treated differently. Since it is possible that interferents in the zero air tank may also have contributed to the artifact signal obtained during the artifact tests, only half of the NO and NO<sub>2</sub> artifact signals were attributed to real instrument bias/contamination and were subtracted from the data (but included in estimates of total uncertainty). It should be stressed that NO and NO<sub>2</sub> artifact signals were relatively small compared with typical ambient levels at Sable Island (median measured values: daytime NO, ~ 20 pptv; NO<sub>2</sub>, ~ 70 pptv). NO<sub>y</sub> artifact signals, however, were subtracted in their entirety from the data as contamination by metal carbonyls from a dirty CO source at the beginning of the campaign was indicated.

For maintenance of the instrument the photolysis cell was first washed with a solution of 5% NaOH and then rinsed with deionized water (Baxter Scientific Products). The gold catalytic converter was heated to 550°C with a flow of zero air of 1 slpm for about 5 hours, followed by three additional hours of flow during the catalyst cooling-down period [see *Hübler et al.*, 1992]. The gold-plated inlet was also heated to 150°C with a flow of zero air of 0.5 slpm. These relatively simple procedures seemed to be effective in keeping the photolysis cell clean and the efficiency of the catalytic converter high with respect to NO<sub>2</sub>.

Detection limits (signal to noise ratio = 2) for NO, NO<sub>2</sub>, and NO<sub>y</sub> were calculated to be 2 pptv, 9 pptv and 3 pptv, respectively, for 2-min integrations. The precision for levels well above detection limits was  $\pm 10\%$ ,  $\pm 17\%$ , and  $\pm 2\%$  for NO, NO<sub>2</sub>, and NO<sub>y</sub>, respectively. The precision estimate is based on photon-counting statistics and is calculated according to the following ambient levels: NO ~ 20 pptv, NO<sub>2</sub> ~ 55 pptv and NO<sub>y</sub> ~ 290 pptv. Overall uncertainties in the measurements were estimated to be (-35%, +28%) for NO, (-39%, +33%) for NO<sub>2</sub>, and (-41%, +36%) for NO<sub>y</sub> (calculated also for above ambient levels). They included the precision and the uncertainties in artifact, the NO calibration standard (2%), the NO<sub>y</sub> conversion efficiency (15%) [*Hübler et al.*, 1992], and mass flowmeter calibrations. In this study, the change in the precampaign and postcampaign sample mass flowmeters cali-

brations (up to 18%) greatly exceeded those previously observed. Because we were not able to determine whether this was a step or a gradual change, interpolated values were used to determine sample flows in the data reduction.

It should be emphasized that accurate determination of total uncertainty in NO<sub>y</sub> measurements is difficult because of the complex issues involved in the measurements, such as converter efficiency, converter poisoning, artifact, and interference from non-NO<sub>y</sub>, nitrogen-containing compounds [*Crosley*, 1994]. Sea salt may cause problems for NO<sub>y</sub> measurements: it may poison the Au catalyst causing drops in conversion efficiencies; it may remove HNO<sub>3</sub> within the inlet if sea-salt deposition occurs in the inlet. Such removal of HNO<sub>3</sub> depends on ambient humidity. In the present study, although we could not be absolutely sure, there seemed no indication of converter poisoning by sea salt at Sable Island (NO<sub>2</sub> conversion efficiencies were > 95% and HNO<sub>3</sub> conversion efficiencies were also believed to be high, as discussed previously). Concerning the removal of HNO<sub>3</sub> within the inlet, we hoped to reduce this problem by heating the inlet to 100°C. However, the effectiveness of this approach was not evaluated in the field. Postcampaign tests on HNO<sub>3</sub> were conducted using dry cylinder air. It should be noted that this measurement site is not in the immediate sea spray zone where the sea-salt problems were discovered.

Artifacts found in this study were quite high and variable, which were mainly attributed to carbonyl compounds in the CO cylinder and to outgassing from the converter and/or sampling line. Although each zero air test could determine the artifact signal accurately at a particular time, linearly interpolated values between the two adjacent artifacts (24-48 hours apart) may introduce errors because (1) two adjacent artifact tests may be not close enough in time for linear interpolation to represent the artifacts between the two tests, especially when the two individual artifact tests differed significantly (e.g., after the HNO<sub>3</sub> test), and (2) change of artifact with time may not follow a straight line. In this uncertainty estimate we included an uncertainty of 5% from artifact determination (relative to ambient NO<sub>y</sub> level of 290 pptv), or 15 pptv. This quantity may have been underestimated for the period immediately after the HNO<sub>3</sub> test in the field (early morning on September 1) but seemed reasonable for the rest of the study period.

The instruments, controlled by a computer, were repetitively switched among zero (instrument background), measurement, and calibration modes. Instrument backgrounds were determined every 30 min. The NO<sub>x</sub> and NO<sub>y</sub> instruments were configured to allow maximum overlap of measurement modes. In the NO<sub>x</sub> instrument, NO and NO<sub>2</sub> measurement modes (each lasting 138 s) alternated between zero modes (each lasting 138 s). The NO<sub>y</sub> instrument had a single measurement mode between zeros. After each transition between modes, 18 s of data were discarded to allow for signal equilibration. The remaining data were averaged over 1-min intervals, and data presented in this paper are 5-min averages.

The following procedures were employed to finalize the data: (1) The data were corrected for artifacts, as described earlier, and for zero-volume efficiency which arises from incomplete conversion of NO in the zero volume by O<sub>3</sub>. Zero-volume efficiency was determined during each artifact test. It should be mentioned that this zero-volume efficiency is very close to unity for the two detectors (0.979 and 0.997, respectively). (2) Interference with the NO<sub>2</sub> measurement, resulting

from the reaction  $\text{NO} + \text{O}_3 \rightarrow \text{NO}_2 + \text{O}_2$  in the photolysis cell, was evaluated during each calibration sequence by determining the detector response when the photolysis cell was bypassed. The subsequent correction lowers NO<sub>2</sub> mixing ratios. However, the magnitude of change of the data resulting from this correction never exceeded 10% and was typically less than 5%. (3) Data associated with periods of instrument malfunction were removed (< 1% of data). (4) Data associated with local pollution were removed (e.g., exhaust from the power generator and passing vehicles). About 11% of the data were excluded for this reason. (5) A wind speed filter was applied and data were removed during periods when the wind speed was less than 1 m/s (~ 2% of the data). This was done to minimize the contamination of the air samples by possible outgassing of the building. (6) Residual signals from the calibration standards were removed. In the NO<sub>x</sub> instrument, a residual signal often existed at a level of ~ 4 pptv after each calibration. Thus NO and NO<sub>2</sub> data obtained during the first 10 min following calibrations were removed. Approximately 7% of NO and 5.3% of NO<sub>2</sub> were excluded. Since ambient NO<sub>y</sub> levels at Sable Island were much higher than the calibration residual, such that no residual was clearly detected, this correction was not applied to the NO<sub>y</sub> mixing ratios.

Prior to the Sable Island experiment, an informal intercomparison of NO<sub>x</sub> and NO<sub>y</sub> measurements was conducted at Chebogue Point, Nova Scotia. Groups from the NOAA Aeronomy Lab, the University of Maryland, and the University of Michigan participated. The data from the Aeronomy Lab (AL) and the University of Michigan (UM) groups were compared. The primary conclusions from the NO<sub>x</sub> intercomparison are (1) the two measurement sets are very well correlated for both NO and NO<sub>2</sub> over the observed concentration range; (2) UM values are about 20% higher than AL values for both species; and (3) the measurements show no significant offsets for either species. The primary conclusions for NO<sub>y</sub> are (1) the Chebogue Point site was particularly poor for intercomparison due to the interferents (presumably ammonia) from the adjacent dairy farm and many spikes in NO<sub>x</sub> and NO<sub>y</sub>; (2) the two data sets are fairly well correlated at least above 2 ppbv; (3) the UM data are about 11% higher than the AL data; and (4) the UM data may be positively offset relative to the AL data below 2 ppbv. Overall, the agreement between the UM and the AL data was found to be good; the systematic differences between the two instrument sets can be attributed to inconsistencies between the UM and the AL calibration standards and to uncertainties associated with UM's mass flowmeter calibrations.

### 3. Results and Discussion

Measurements of reactive nitrogen (NO, NO<sub>2</sub>, and NO<sub>y</sub>) started on the evening of August 14 and ended on the early morning of September 6. Daytime temperatures during the study period were mild with an average value of 18°C and a diurnal difference of about 2°C. Relative humidity was typically high, averaging 80% during the day and near 100% at night. Southwesterly winds slightly predominated; wind speed averaged around 3.7 m/s with no strong diurnal variation.

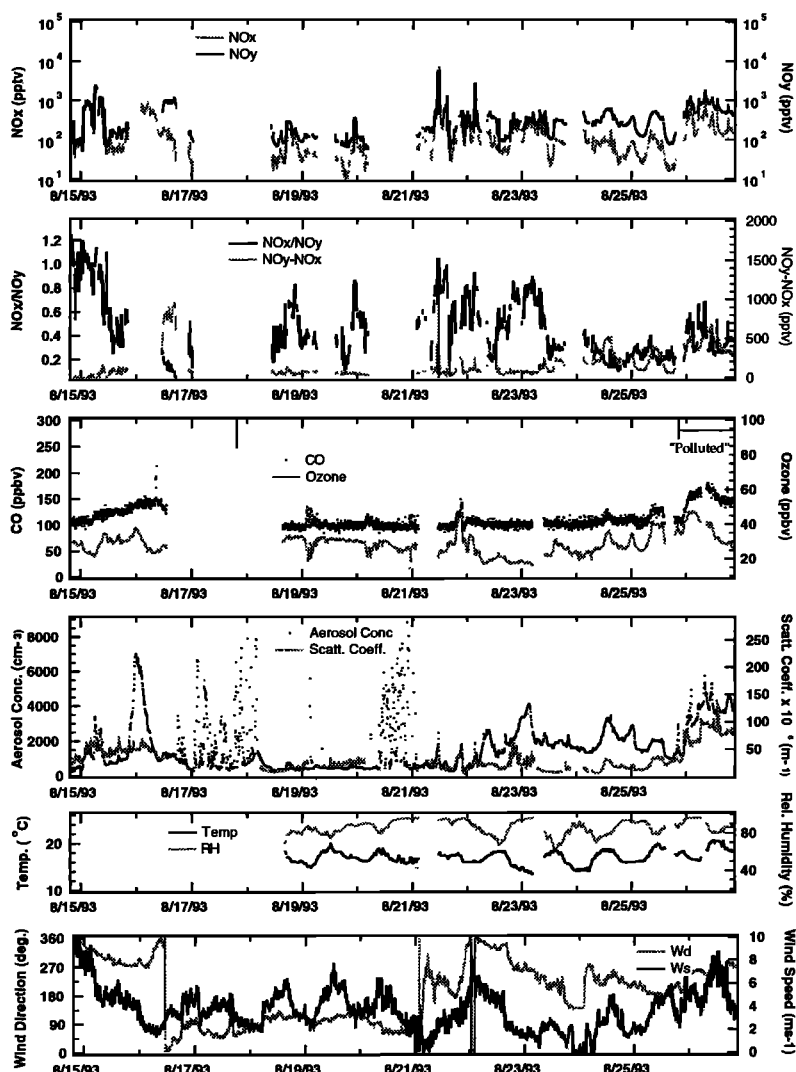
Figure 3 shows the time series of NO<sub>x</sub>, NO<sub>y</sub>, NO<sub>x</sub>/NO<sub>y</sub>, oxidation products of NO<sub>x</sub> (NO<sub>y</sub>-NO<sub>x</sub>), CO, O<sub>3</sub>, aerosol number concentration, scattering coefficient, temperature, relative humidity, wind speed, and wind direction. Aerosol number

concentrations were determined for particles greater than 15 nm in diameter (TSI, model 3760 CNC). Scattering coefficients (at wavelength of 550 nm) were measured at relative humidity of less than 30% and for particles less than 10 μm in diameter. Three large time gaps in the reactive nitrogen time series indicate the periods when air sampled at the site was contaminated by exhaust from the island generator, during which the instruments were switched from ambient air to zero air. These three periods are August 16-18, August 20-21, and September 2-3.

In general, levels of NO<sub>x</sub>, NO<sub>y</sub>, and to a lesser extent condensation nuclei exhibited variations on a relatively short timescale, whereas CO, O<sub>3</sub>, and aerosol scattering coefficient varied on a much longer timescale (an example can be seen on August 22-23). Additionally, the magnitude of changes relative to mixing ratios of NO<sub>x</sub> and NO<sub>y</sub> are much more pronounced than for the other species (here, logarithm scales are adopted for the NO<sub>x</sub> and NO<sub>y</sub> axes). Quite often, increases in NO<sub>x</sub> and NO<sub>y</sub> mixing ratios were observed without concurrent enhancements in CO levels, and often aerosol concentrations showed enhancements during these NO<sub>x</sub> and NO<sub>y</sub> peaks. An example of these events can be seen around noon on August 21. Typically, these peaks in NO<sub>y</sub> levels lasted from a half hour to several hours and such periods occurred throughout this study. The ratio of NO<sub>x</sub> to NO<sub>y</sub> is found to increase during these NO<sub>x</sub> and NO<sub>y</sub> peaks, which suggests that reactive nitrogen observed during these periods may have come from relatively fresh sources in the area. Exhaust from the island generators could contaminate air samples measured at the site in two ways: (1) an air parcel carrying pollutants to the site sampled shortly after contamination and (2) an air parcel carrying pollutants that had been transported away from the site for some time and returned to the site due to a change in the flow pattern. However, the chemical and surface wind data associated with these peak events were examined, and no indication that the air sampled during these periods had been contaminated by the island generators was found. Instead, sources upwind of Sable Island (e.g., ship exhaust and emissions from the oil production facility) may have contributed to these observed peaks. This speculation is supported by the fact that diesel generators at the oil production platform and diesel engines that are widely used on ships tend to burn fuel efficiently, discharging exhaust with high NO<sub>x</sub> to CO ratios and large amount of particles. Additionally, a least one radio contact was made by the Sable Island Weather Station during an NO<sub>y</sub> peak event, and there was indeed a ship passing the island upwind of the measurement site. Surface wind, reactive nitrogen, and aerosol concentration data were examined in an attempt to find particular wind direction window(s) in which these sources appear dominant. These sources appeared to exist in all wind directions except for easterly and southeasterly flows (data associated with northeasterly flows were contaminated by the generators).

Although the levels of reactive nitrogen sometimes varied independently of CO and ozone, there were periods when reactive nitrogen, CO, and ozone were correlated. For example, on August 24-26, NO<sub>y</sub>, CO, and O<sub>3</sub> levels all varied quite smoothly, exhibiting three maxima for a 36-hour period. It is also noteworthy that during this period, NO<sub>x</sub>/NO<sub>y</sub> remained low and less variable (0.2-0.4).

A major pollution episode occurred from midnight on August 26 to midnight on August 29. During this period, NO<sub>x</sub>, NO<sub>y</sub>, CO, O<sub>3</sub>, scattering coefficient, and condensation nuclei



(a) August 14 - August 26

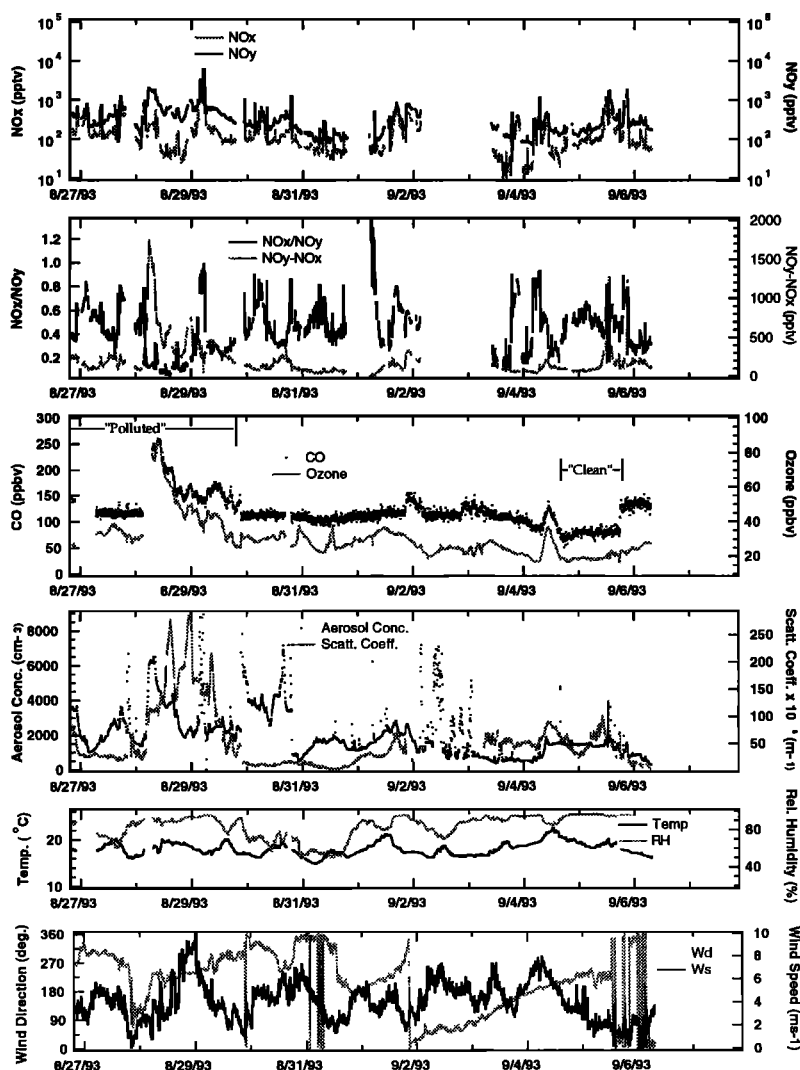
**Figure 3.** Twelve-day time series of  $\text{NO}_x$ ,  $\text{NO}_y$ , CO,  $\text{O}_3$ ,  $\text{NO}_x/\text{NO}_y$ ,  $\text{NO}_y-\text{NO}_x$ , aerosol concentration (for particles  $> 15$  nm in diameter), scattering coefficient (550 nm,  $\text{RH} < 30\%$ ), temperature, relative humidity, wind speed and wind direction. Note that  $\text{NO}_x$  and  $\text{NO}_y$  are in log scale. Tick marks on the time axes indicate starting of a day (0000), "clean" and "polluted" events (see text in the later section for definitions) are marked in CO time series.

as well as nonmethane hydrocarbon species (not shown) showed significant enhancements. For example, ozone reached at least 85 ppbv and CO at least 250 ppbv on the morning of August 28;  $\text{NO}_y$  mixing ratios were as high as 1700 pptv (median value for this study, 266 pptv). The ratio of  $\text{NO}_x$  to  $\text{NO}_y$  was less than 0.1 in the afternoon of that day, suggesting that the air parcel was well aged in terms of the degree of photochemical processing. This event is referred to in this paper as the "polluted" event. Four-day isentropic back trajectories calculated by J. Moody suggest that the air mass traveling over Sable Island during the pollution episode may have come from the highly industrialized northeastern and/or midwestern United States. During the same period, surface winds at Sable Island were also from southwest. It should be mentioned here that these back trajectories were calculated for altitudes usually much higher than the sampling height and as a result vertical stratification may limit their application to

this data set (see Angevine *et al.*, [this issue], for details). Indications of stratification will be discussed below in this paper. Another interesting feature during the pollution episode is worth mentioning:  $\text{NO}_y$  (as well as  $\text{NO}_y-\text{NO}_x$ ) and condensation nuclei reached their peak levels around 0300 on August 28 and then showed a rapid decrease, whereas CO and  $\text{O}_3$  remained rather constant and then showed a slower decrease. We attribute this behavior to the removal of relatively soluble species such as  $\text{HNO}_3$ , aerosol nitrate, and condensation nuclei along the air mass trajectory. Carbon monoxide and  $\text{O}_3$  are less affected by this type of removal process. This phenomenon is discussed below and is also addressed by Roberts *et al.* [this issue].

In contrast to the pollution episode, air masses with different characteristics were sampled for a 36-hour period on September 4–5 following the passage of Hurricane Emily. The air was characterized by low and stable levels of CO ( $\sim 80$





(b) August 27 - September 6

Figure 3. (continued)

ppbv) and ozone ( $\sim 15$  ppbv). Mixing ratios of reactive nitrogen, however, were quite variable. Again the existence of relatively fresh sources of reactive nitrogen can be seen. In this paper we refer to this period as the "clean" event, which will be examined in greater detail below. Local surface winds were south-southwesterly and back trajectory calculations suggest that air traveling over Sable Island during this "clean" event originated in the tropical Atlantic Ocean.

If the "polluted" and "clean" episodes are excluded, the remaining data may represent "regional" background conditions. This category accounts for the majority of the data collected in this study.

Vertical stratification in the marine boundary layer is an issue. There is evidence that vertical mixing at Sable Island was limited. Each day, at 0815 and 2015 (Atlantic standard time), radiosondes (VIZ Canada, model: VIZ RAP) were launched by Atmospheric Environment Service (AES) staff as part of their normal operation. The radiosondes showed vertical profiles that primarily indicated stable or neutrally stable conditions within the marine boundary layer during launching times throughout the study. Figure 4 shows typical profiles of

potential temperature and water vapor mixing ratio. Although no sounding information is available at noon or in the early afternoon when surface heating-induced vertical mixing tends to be maximum, surface temperature data suggest that surface heating by solar radiation was small (average and maximum afternoon temperature is  $\sim 18^\circ\text{C}$  and  $20^\circ\text{C}$ , respectively; and diurnal difference is only  $\sim 2^\circ\text{C}$ ). Further evidence for the lack of vertical mixing comes from a direct comparison of chemical measurements made by the overflying aircraft with surface measurements. These results are presented in a later section. In short, surface levels of  $\text{O}_3$ , CO, and  $\text{NO}_y$  were quite different from those at altitudes as low as 300 m, indicating the existence of vertical stratification. Additional discussion of the vertical sounding data is presented by M. A. Carroll et al. (manuscript in preparation, 1996).

Frequency distributions of  $\text{O}_3$ , CO,  $\text{NO}_x$ , and  $\text{NO}_y$  are shown in Figure 5. For each species the "polluted" event (August 25, 2146 AST – August 29, 1752 AST), the "clean" event (September 4, 1602 AST– September 5, 1752 AST), and the "rest" of the data are shown separately. From the CO and  $\text{O}_3$  distributions, one can see that during the "clean" event both

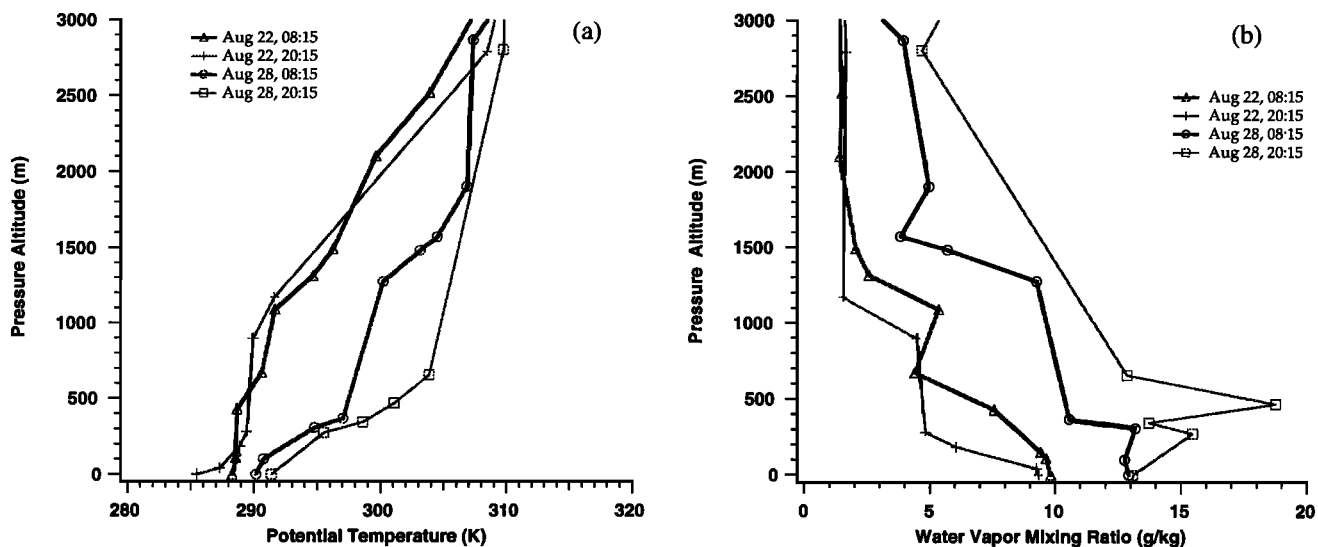


Figure 4. Typical vertical profiles of (a) potential temperature and (b) water vapor mixing ratio, as derived from radiosonde data.

ozone and CO levels were low and the median mixing ratios were 19 and 78 ppbv, respectively. The mean values for  $\text{O}_3$  and CO mixing ratios in this subdata set are 19 ppbv and 79 ppbv, respectively. Their histograms are approximately represented by a Gaussian distribution. In the "polluted" case, however, both  $\text{O}_3$  and CO levels are much higher than in the "clean" case. Median mixing ratios are 38 ppbv and 147 ppbv for  $\text{O}_3$  and CO, respectively. The majority of data collected during the study falls in the "rest" category which has a median of 27 ppbv and 108 ppbv for  $\text{O}_3$  and CO, respectively. These distributions lie between those of the "clean" and "polluted" cases.

For reactive nitrogen the above grouping approach is not so obvious as it is for ozone and CO. For example, even in the "clean" event, both  $\text{NO}_x$  and  $\text{NO}_y$  were highly variable in their respective levels. Although the median mixing ratio of  $\text{NO}_y$  is 189 pptv, the mean value is 321 pptv and 4.6% of the data in

this category exceed 1000 pptv.  $\text{NO}_x$  showed a similar distribution with a median of 98 pptv and a mean of 153 pptv. This suggests the existence of sources characteristic of high  $\text{NO}_x$  to CO ratios in the area that contribute to the reactive nitrogen levels observed at Sable Island. Evidence of these sources can be seen in all three subdata sets. The pollution episode was responsible for the extremely high concentrations of  $\text{O}_3$  and CO, but this does not hold true in the case of reactive nitrogen.

Therefore the general picture is that at Sable Island the variability of CO and  $\text{O}_3$  seems to be determined by the long-range transport of air masses with different histories, whereas the levels of  $\text{NO}_x$  and  $\text{NO}_y$  are primarily determined by the sources within relatively short distances. This may be a feature characteristic of the western North Atlantic, and the impact of these sources on the regional ozone budget needs to be further assessed.

Diurnal distributions of NO,  $\text{NO}_2$ ,  $\text{NO}_x$ ,  $\text{NO}_y$ ,  $\text{NO}_x/\text{NO}_y$ ,

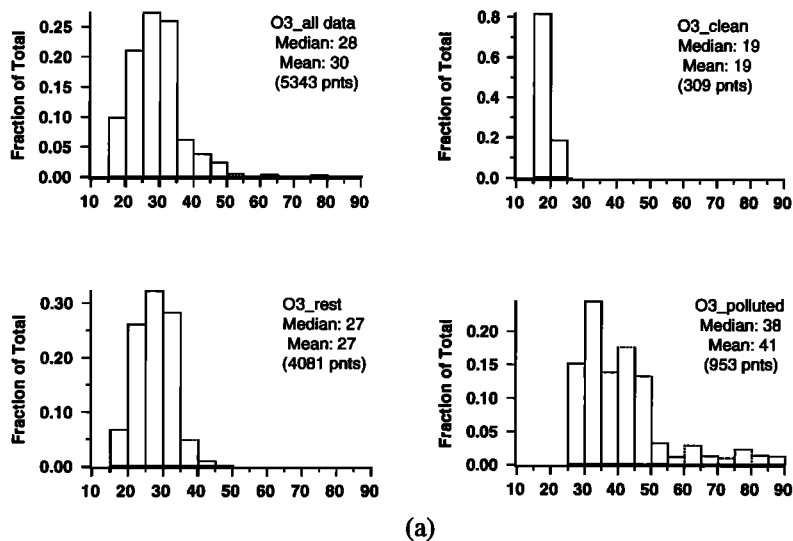
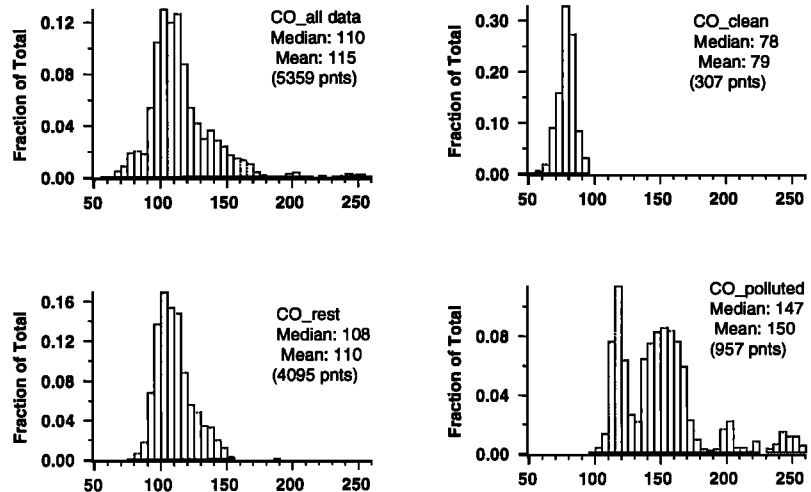
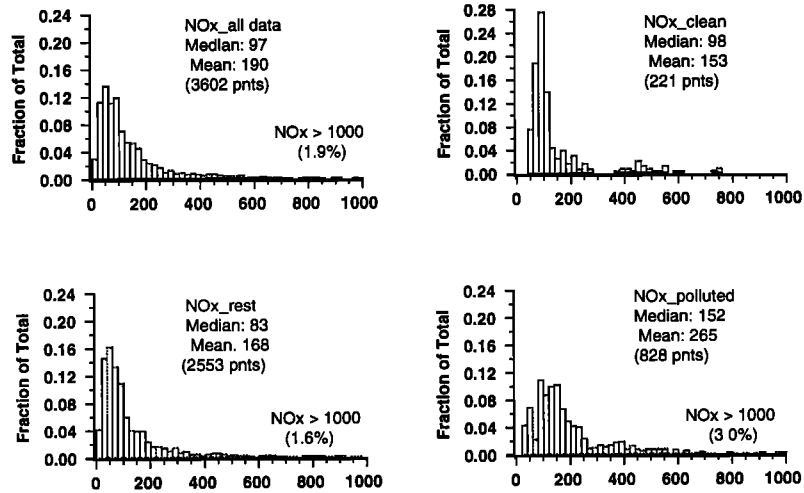


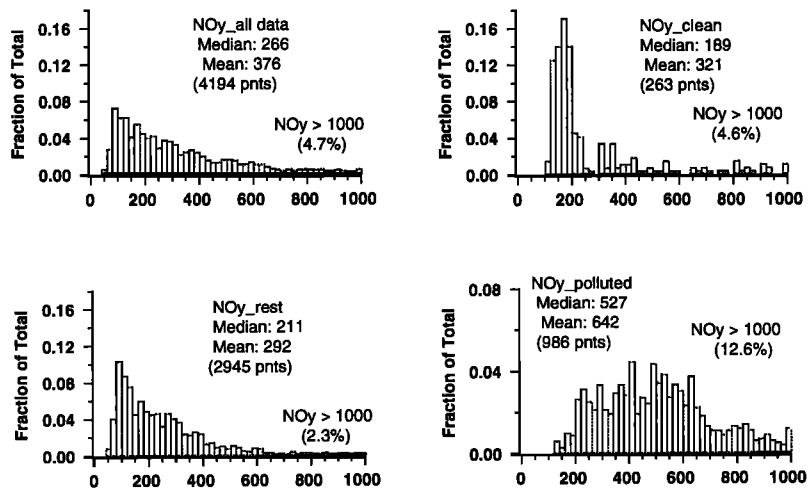
Figure 5. Frequency distributions for (a)  $\text{O}_3$ , (b) CO, (c)  $\text{NO}_x$  and (d)  $\text{NO}_y$ . For each species the entire data set, the "polluted" event, the "clean" event, and the "rest" of the data (excluding the polluted and clean events) are shown. See text for their definitions.



(b)



(c)



(d)

Figure 5. (continued)

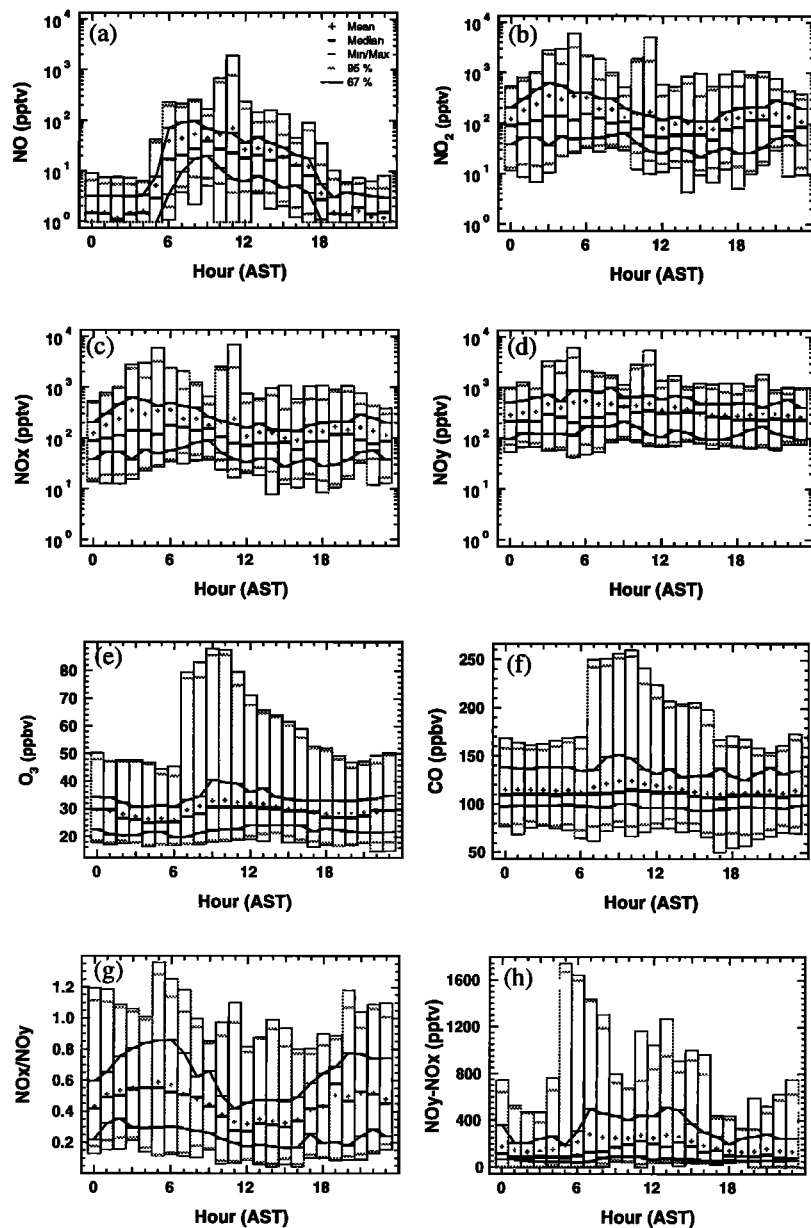


**Figure 6.** Hourly averaged diurnal distributions, including maximum, minimum, central 95%, central 67%, mean, and median values for (a) NO, (b) NO<sub>2</sub>, (c) NO<sub>x</sub>, (d) NO<sub>y</sub>, (e) O<sub>3</sub>, (f) CO, (g) NO<sub>x</sub>/NO<sub>y</sub>, and (h) NO<sub>y</sub>-NO<sub>x</sub>.

NO<sub>y</sub>-NO<sub>x</sub>, CO, and O<sub>3</sub> are presented in Figure 6. Shown are hourly averaged values, medians, central 67%, central 95%, and range. The increase in the difference between means and medians in the case of ozone and CO is primarily due to the fact that during the pollution episode, CO and O<sub>3</sub> peaked between 0800 am and 1200 AST on the morning of August 28. Thus extremely high concentrations in that single incident resulted in skewed distributions. This is also true for reactive nitrogen, NO<sub>x</sub> and NO<sub>y</sub>. However, the largest difference between the means and the medians of NO<sub>x</sub> and NO<sub>y</sub> occurs at earlier morning hours than those associated with O<sub>3</sub> and CO, as a result of the fact that both NO<sub>x</sub> and NO<sub>y</sub> peaked around 0600 AST, whereas CO and O<sub>3</sub> data peaked around 1000 (there is no data record of ozone and CO between 0300 to 1000 on August 28). Thus in a discussion of diurnal behavior our focus is on the median and central 67% of the data since they are less affected by the small number of extreme values.

Carbon monoxide levels did not have an obvious diurnal cycle and the median mixing ratio remained ~ 110 ppbv throughout a diurnal period. Ozone showed some diurnal behavior, with a broad maximum around local noon (1100 AST) and a minimum in the morning around 0600 AST. However, the degree of enhancement at noon and depression during the early morning in O<sub>3</sub> levels was much less than that observed at the surface sites in the continental boundary layer [e.g., Parrish *et al.*, 1993b]. The smaller early morning decrease as compared with that at continental surface sites may be attributed to the combination of the following processes in this marine boundary layer site: (1) less vigorous development of nocturnal inversion which allows some transport of ozone aloft; (2) advection that transports the ozone over the ocean at night. Here, horizontal transport of ozone at night is supported by the surface wind observations which suggests that wind speed often remained constant from daytime to

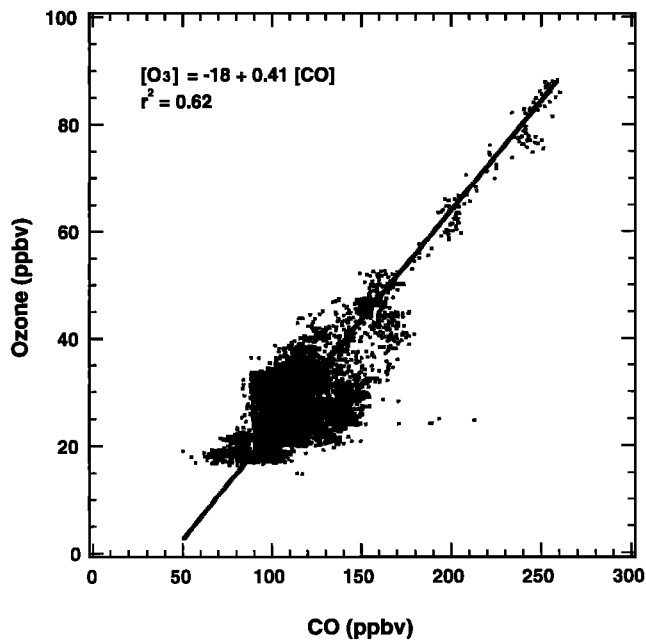


Figure 7. Ozone mixing ratio versus CO mixing ratio.

nighttime. The noon/afternoon maximum is also smaller at this site, which may be attributed to weaker local photochemical production of ozone, and/or less vigorous transport of ozone from ozone rich regions aloft during daytime.

A diurnal variation of median NO<sub>y</sub> may exist, as daytime values (~ 270 pptv) were typically larger than those at night (~ 220 pptv). The median NO<sub>x</sub> showed the opposite diurnal trend, with daytime values generally lower than nighttime values. The combination of these two opposite diurnal trends resulted in a distinct diurnal pattern in the NO<sub>x</sub>/NO<sub>y</sub> ratio whose median was around 0.3 during the daytime and about 0.5 at night. The NO<sub>y</sub> diurnal trend can be explained by one or a combination of the following two processes: (1) stronger transport during daytime, presumably through some degrees of downward mixing of NO<sub>y</sub> rich air masses; and (2) stronger removal of NO<sub>y</sub> components such as HNO<sub>3</sub> and aerosol nitrate at night. Photochemical conversion of NO<sub>x</sub> to HNO<sub>3</sub> may contribute to the daytime decrease of NO<sub>x</sub> levels. The diurnal cycles of NO and NO<sub>y</sub>-NO<sub>x</sub> are as expected, with maxima occurring during the daytime and minima at night.

The relationship of reactive nitrogen species with CO and O<sub>3</sub> can provide valuable information on source origin, transport, photochemical transformation and physical removal processes involving these species. As discussed by Fehsenfeld *et al.* [this issue (a)], a previous study conducted by Parrish *et al.* [1993a] found that the ozone correlated well with CO, an anthropogenic tracer, at three surface sites near the Atlantic Coast of Canada (Sable Island was one of the sites) and concluded that elevated ozone is produced from precursors of anthropogenic origin, i.e., NO<sub>x</sub> and volatile organic compounds (VOCs). Figure 7 shows the correlation plot between ozone and CO obtained during the present study. Here, the relation between these two species was found to be similar to that observed in the previous study. For example, the slope ( $\Delta[\text{O}_3]/\Delta[\text{CO}]$ ) is 0.41 in this study, versus 0.30 obtained previously; the correlation coefficient is 0.62 versus 0.68. However, it is noted that the observed correlation in this study is driven primarily by a single pollution episode

resulting from the transport of pollutants from the North American continent, whereas in the previous study, multiple pollution events were observed.

If elevated levels of O<sub>3</sub> are a result of photochemistry involving anthropogenic precursors and if both ozone and reactive nitrogen undergo similar physical (dilution and removal) processes, a positive correlation between ozone and NO<sub>y</sub>-NO<sub>x</sub> would be expected. Such a relation has been observed in many places over the North American continent [e.g., Trainer *et al.*, 1993; Olszyna *et al.*, 1994; Kleinman *et al.*, 1994]. However, as shown in Figure 8, a simple correlation between ozone and NO<sub>y</sub>-NO<sub>x</sub> obtained from the present study is not obvious. Both daytime and nighttime data are included in this figure since there is no strong diurnal cycle of boundary layer development such as impacts nighttime ozone levels at continental sites. It is worth mentioning that the data points associated with ozone mixing ratios higher than 50 ppbv are from the peak period of the pollution episode on August 28. Here, we see indications of the removal of reactive nitrogen from the air parcels arriving at the site. For example, at about 0740 AST, mixing ratios of NO<sub>y</sub>-NO<sub>x</sub>, O<sub>3</sub>, and NO<sub>x</sub> were 1440 pptv, 77 ppbv, and 232 pptv (NO<sub>x</sub>/NO<sub>y</sub> = 0.14), respectively. At about 1021, their respective levels became 660 pptv, 86 ppbv, and 72 pptv (NO<sub>x</sub>/NO<sub>y</sub> = 0.10). NO<sub>y</sub>-NO<sub>x</sub> dropped by more than a factor of 2 and NO<sub>x</sub> levels decreased by a factor of 3, while O<sub>3</sub> levels rose slightly. The decrease of total reactive oxidized nitrogen (NO<sub>y</sub>) in the second air parcel must have resulted from its removal, if one assumes that the two air parcels had similar initial loading of anthropogenic emissions. This assumption is partially supported by the observation of similar levels of CO (~ 250 ppbv) in the two air parcels and by the fact that fog was present at Sable Island during the peak episode up until noon on August 29. An indication of NO<sub>y</sub> removal can also be seen in the correlation plot of NO<sub>y</sub> with O<sub>3</sub>. If one forces a linear fit (two sided) to the data, the obtained slope ( $\Delta[\text{O}_3]/\Delta[\text{NO}_y\text{-NO}_x]$ , ppbv/ppbv) is 86 ( $r^2 = 0.41$ ), which is much higher than the slopes from regression analyses applied to observations obtained in continental

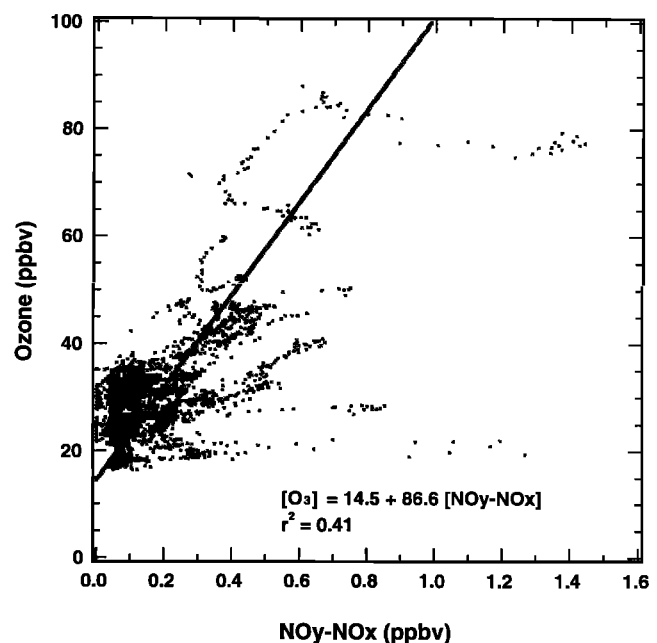


Figure 8. Ozone mixing ratio versus NO<sub>y</sub>-NO<sub>x</sub> mixing ratio.

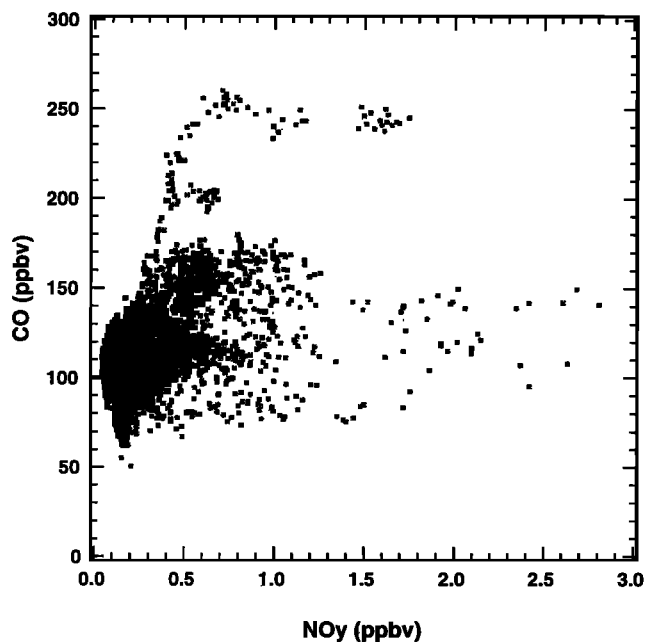


Figure 9. CO mixing ratio versus NO<sub>y</sub> mixing ratio.

North America (6 - 13) [e.g., *Trainer et al.*, 1993; *Olszyna et al.*, 1994; *Kleinman et al.*, 1994] and from model calculations (~ 4) [*Jacob et al.*, 1993; *Chin et al.*, 1994]. Again, the much larger slope observed in this experiment can be attributed to the relatively short lifetime of NO<sub>y</sub> due to its removal in the marine boundary layer. Similar observations were also made at Chebogue Point, and potential loss mechanisms are further considered by *Roberts et al.* [this issue].

The correlation of NO<sub>y</sub> with CO is shown in Figure 9. Here, a simple linear correlation does not exist. The NO<sub>y</sub> axis is set to exclude the data points for NO<sub>y</sub> > 3000 pptv (14 points) in order to focus on levels typically observed. The relationship between these two species is complicated not only by NO<sub>y</sub> removal processes likely represented by the data in the top left-hand corner of the graph but also by the relatively fresh emissions of NO<sub>x</sub> discussed throughout the text, likely represented by the data in the bottom right-hand corner of the graph.

Finally, an important unresolved issue in the field of atmospheric chemistry concerns the validity and limitation of surface measurements in the marine boundary layer in addressing science questions that are regional in nature. This is especially of concern because of the stratification frequently indicated in the marine environment. Comparing surface measurements with those made by overflying aircraft is valuable. During the experiment, three instrumented aircraft flew over or near Sable Island at different altitudes. In this paper, measurements onboard the Gulf Stream-1(G-1) and the King Air aircraft are compared with the surface measurements. Table 1 summarizes the results from this comparison.

Case 1. On August 22, between 1212 and 1222 AST, the G-1 flew over Sable Island. The conditions were warm and sunny: surface Eppley radiometer data show that the site received full solar radiation, and the maximum daytime temperature was ~ 18°C. In addition, the radiosonde launched around 0800 AST indicated neutral stability near the surface (Figure 4), leading to the speculation that air might have become unstable in the

afternoon. The G-1 flew over the site at an altitude of about 160 m. Mixing ratios of surface O<sub>3</sub>, CO, and NO<sub>y</sub> are comparable to their respective values at 160 m altitude. However, according to the aircraft data, both ozone and CO concentrations increase with altitude: ozone increasing from 24 to 43 ppbv and CO from 85 to 143 ppbv, with altitude changes from 300 to 1500 m. These observations may indicate that local mixing only extended throughout the lowest few hundred meters or that vertical stratification resulted in stable layers, including one just above the site.

Case 2. The G-1 flew over the island on August 25 around 0930 AST at an altitude of ~ 340 m. The daytime temperature was approximately 19°C and it was sunny in the morning and became cloudy in the afternoon. Surface ozone data agreed with the aircraft data although there appeared to be some finer structure in the ozone vertical profile between the surface and the 340-m level. There are large differences in the CO and NO<sub>y</sub> mixing ratios between the surface and the 340-m level; upper level values are much higher than those at the surface.

Case 3. The King Air flew near Sable Island around 1134-1154 AST on August 28 at an altitude of about 400 m. The daytime maximum temperature was 19-20°C, and it became cloudy in the afternoon. Vertical sounding (Figure 4) indicated stable condition around launching time. Again surface levels of O<sub>3</sub>, CO and NO<sub>y</sub> are much lower than those at ~ 400 m.

In summary, there are clear indications of vertical stratification above the site in all three cases examined.

#### 4. Conclusions

NO, NO<sub>2</sub>, and NO<sub>y</sub> were measured at Sable Island from August 14 to September 6 during the NARE 1993 summer intensive. NO<sub>x</sub> and NO<sub>y</sub> levels were found to be highly variable, whereas CO and O<sub>3</sub> showed much less variability. The medians for NO<sub>x</sub> and NO<sub>y</sub> were 98 and 266 pptv, respectively.

Table 1. Airborne Versus Ground-Based Measurements

	O <sub>3</sub> , ppbv	CO, ppbv	NO <sub>y</sub> , pptv
<i>Case 1</i>			
G-1	20 - 24 (22)*	75 - 125 (NA)	300 - 450 (400)
Ground	21 - 21 (21)	98 - 103 (100)	333 - 356 (333)
<i>Case 2</i>			
G-1	41 - 62 (42)	120 - 180 (180)	1200 - 1800 (1800)
Ground	40 - 41 (41)	126 - 128 (128)	498 - 500 (500)
<i>Case 3</i>			
King Air	80 - 130	210 - 290	6000 - 20000
Ground	72 - 73	224 - 233	462 - 475

Case 1, August 22, 1212-1222 AST, ~ 160 m, overflight by G-1 [*Kleinman et al.*, this issue]; case 2: August 25, 0929-0939 AST, ~ 340 m, overflight by G-1 [*Kleinman et al.*, this issue]; case 3: August 28, 1134-1154 AST, ~ 400 m, near flight by King Air [*Buhr et al.*, this issue].

\* Numbers in parentheses are mixing ratios at the time approximately when aircraft flew over the island.

Elevated levels of reactive nitrogen can be attributed to the transport of polluted continental air or presumably to relatively fresh emissions from sources upwind (e.g., ship exhaust). A multiday pollution episode occurred on August 26-29, and air masses of recent tropical marine origin characterized by low and constant levels of CO and O<sub>3</sub> were sampled on September 4-5.

Ozone correlated reasonably well with CO, although the correlation is primarily driven by the single pollution episode. The correlation between ozone and NO<sub>y</sub>-NO<sub>x</sub> is complicated, and  $\Delta[\text{O}_3]/\Delta[\text{NO}_y\text{-NO}_x]$  is much higher than those values obtained from continental studies. This result is primarily attributed to the removal of NO<sub>y</sub> along the air mass trajectory. An indication of the removal of NO<sub>y</sub> was seen on the morning of August 28, when NO<sub>y</sub> levels dropped by more than a factor of 2 while CO and O<sub>3</sub> remained at elevated levels.

By comparing results from the surface and overflying aircraft measurements, we found clear indications of vertical stratification. Studies under way include the estimation of peroxy radical levels and photochemical production and loss of ozone (K. A. Duderstadt et al., manuscript in preparation, 1996), further characterization of air mass origin focusing on transport within the marine boundary layer and correlation analyses for origin categories and specific air parcels (M. A. Carroll et al., manuscript in preparation, 1996), and removal mechanisms for reactive nitrogen in the marine environment.

**Acknowledgments.** The authors would like to thank the staff at the Sable Island Weather Station for its excellent logistical support. Thanks to D. D. Parrish for providing the gold catalytic converter assembly, G. Hübler for providing the HNO<sub>3</sub> permeation source and CO cylinders, S. Beauchamp of the Canadian Atmospheric Environment Services for his assistance in getting the information on ship traffic and meteorological data, P. Daum for providing G-1 overflight data, M. Buhr for providing King Air data, N. Blake for providing the hydrocarbon data, J. Moody and J. Merrill for providing calculated back trajectories, L. Emmoms for preparing the map of Sable Island, F. Marsik for his help in the meteorological analysis, and S. Sillman for his helpful comments. This research was supported by the Atmospheric Chemistry Component of the NOAA Climate and Global Change Program.

## References

- Angevine, W., M. Trainer, S. McKeen, and C. M. Berkowitz, Mesoscale meteorology of the New England coast, Gulf of Maine, and Nova Scotia, *J. Geophys. Res.*, this issue
- Atlas, E. L., B. A. Ridley, G. Hübler, M. A. Carroll, D. D. Montzka, B. Huebert, R. Norton, J. G. Walega, F. Grahek, and S. Schauffler, Partitioning and budget of NO<sub>y</sub> species during Mauna Loa Observatory Photochemistry Experiment, *J. Geophys. Res.*, **97**, 10,449-10,462, 1992.
- Buhr, M. D., Sueper, M. Trainer, P. Goldan, B. Kuster, and F. Fehsenfeld, Trace gas and aerosol measurements using aircraft data from the North Atlantic Regional Experiment (NARE 1993), *J. Geophys. Res.*, this issue.
- Bollinger, M. J., R. E. Sievers, D. W. Fahey, and F. C. Fehsenfeld, Conversion of nitrogen dioxide, nitric acid, and n-propyl nitrate to nitric oxide by gold-catalyzed reduction with carbon monoxide, *Anal. Chem.*, **55**, 1980-1986, 1983.
- Carroll, M. A., et al., Aircraft measurements of NO<sub>x</sub> over the eastern Pacific and continental United States and implications for ozone production, *J. Geophys. Res.*, **95**, 10,205-10,233, 1990a.
- Carroll, M. A., D. D. Montzka, G. Hübler, K. K. Kelly, and G. L. Gregory, in situ measurements of NO<sub>x</sub> in the Airborne Arctic Stratospheric Expedition, *Geophys. Res. Lett.*, **17**, 493-496, 1990b.
- Carroll, M. A., B. A. Ridley, D. D. Montzka, G. Hübler, J. G. Walega, R. B. Norton, and B. J. Huebert, Measurements of nitric oxide and nitrogen dioxide during the Mauna Loa Observatory Photochemistry Experiment, *J. Geophys. Res.*, **97**, 10,361-10,374, 1992.
- Chameides, W. L., The photochemical role of tropospheric nitrogen oxides, *Geophys. Res. Lett.*, **5**, 17-20, 1978.
- Chin, M., D. J. Jacob, J. W. Munger, D. D. Parrish, and B. G. Doddridge, Relationship of ozone and carbon monoxide over North America, *J. Geophys. Res.*, **99**, 14,565-14,573, 1994.
- Crosley, D. R., Issues in the measurement of reactive nitrogen compounds in the atmosphere: A report on a workshop held at SRI International, December 1993, *Rep. MP 94-035*, NASA, Menlo Park, Calif., 1994.
- Crutzen, P. J., Photochemical reactions initiated by and influencing ozone in unpolluted tropospheric air, *Tellus*, **26**, 47-57, 1974.
- Crutzen, P. J., The Role of NO and NO<sub>2</sub> in the chemistry of the troposphere and stratosphere, *Ann Rev. Earth Planet Sci.*, **7**, 443-472, 1979.
- Doddridge, B. G., R. R. Dickerson, J. Z. Holland, J. N. Cooper, R. G. Wardell, O. Poulida, and J. G. Watkins, Observation of tropospheric trace gases and meteorology in rural Virginia using an unattended monitoring system: Hurricane Hugo (1989), a case study, *J. Geophys. Res.*, **96**, 9341-9360, 1991.
- Fahey, D. W., C. S. Eubank, G. Hübler, and F. C. Fehsenfeld, Evaluation of a catalytic reduction technique for the measurement of total reactive odd-nitrogen NO<sub>y</sub> in the atmosphere, *J. Atmos. Chem.*, **3**, 435-468, 1985.
- Fahey, D. W., G. Hübler, D. D. Parrish, E. J. Williams, R. B. Norton, B. A. Ridley, H. G. Singh, S. C. Liu, and F. C. Fehsenfeld, Reactive nitrogen species in the troposphere: Measurements of NO, NO<sub>2</sub>, HNO<sub>3</sub>, particulate nitrate, PAN, O<sub>3</sub>, and total reactive odd nitrogen (NO<sub>y</sub>) at Niwot Ridge, Colorado, *J. Geophys. Res.*, **91**, 9781-9793, 1986.
- Fehsenfeld, F. C., et al., A ground-based intercomparison of NO, NO<sub>x</sub>, and NO<sub>y</sub> measurement techniques, *J. Geophys. Res.*, **92**, 14,710-14,722, 1987.
- Fehsenfeld, F. C., A. Volz-Thomas, S. Penkett, M. Trainer, and D. D. Parrish, North Atlantic Regional Experiment (NARE) 1993 summer intensive: Foreword, *J. Geophys. Res.*, this issue (a).
- Fehsenfeld, F. C., P. Daum, W. R. Leatch, M. Trainer, D. D. Parrish, and G. Hübler, Transport and processing of O<sub>3</sub> and O<sub>3</sub> precursors over the North Atlantic; An overview of the 1993 NARE summer intensive, *J. Geophys. Res.*, this issue (b).
- Fishman, J., V. Ramanathan, P. J. Crutzen, and S. C. Liu, Tropospheric ozone and climate, *Nature*, **282**, 818-820, 1979.
- Fishman, J., Ozone in the troposphere, in *O<sub>3</sub> in the Free Troposphere*, edited by R. C. Whitten and S. S. Prasad, pp. 161-194, D. Van Nostrand, New York, 1985.
- Fishman, J., and J. C. Larsen, Distribution of total ozone and stratospheric ozone in the tropics: Implications for the distribution of tropospheric ozone, *J. Geophys. Res.*, **93**, 6627-6632, 1987.
- Fishman, J., P. Minnis, and H. G. Reichle, Use of satellite data to study tropospheric ozone in the tropics, *J. Geophys. Res.*, **92**, 14,451-14,465, 1986.
- Fishman, J., C. E. Watson, J. C., Larsen, and L. A. Logan, The distribution of tropospheric ozone determined from satellite data, *J. Geophys. Res.*, **95**, 3599-3617, 1990.
- Hübler, G., et al., Total reactive oxidized nitrogen (NO<sub>y</sub>) in the remote Pacific troposphere and its correlation with O<sub>3</sub> and CO: Mauna Loa Observatory Photochemistry Experiment 1988, *J. Geophys. Res.*, **97**, 10,427-10,447, 1992.
- Jacob, D. J., J. A. Logan, G. M. Gardner, R. M. Yevich, C. M. Spivakovsky, and S. C. Wofsy, Factors regulating ozone over the United States and its export to the global atmosphere, *J. Geophys. Res.*, **98**, 14,817-14,826, 1993.
- Jaffe, D. A., R. E. Honrath, J. A. Herring, S.-M. Li, and J. D. Kahl, Measurements of nitrogen oxides at Barrow, Alaska during spring: Evidence for regional and northern hemispheric sources of pollution, *J. Geophys. Res.*, **96**, 7395-7405, 1991.
- Kleinman, L., Y.-N. Lee, S. R. Springston, L. Nunnermacker, X. Zhou, R. Brown, K. Hallock, P. Klotz, D. Leahy, J. H. Lee, and L. Newman, Ozone formation at a rural site in the southeastern United States, *J. Geophys. Res.*, **99**, 3469-3482, 1994.
- Kleinman, L. I., P. H. Daum, Y.-N. Lee, S. R. Springston, L. Newman, W. R. Leatch, C. M. Banic, G. A. Isaac, and J. I. MacPherson, Measurement of O<sub>3</sub> and related compounds over southern Nova Scotia, I, Vertical distributions, *J. Geophys. Res.*, this issue.
- Liu, S. C., D. Kley, M. McFarland, J. D. Mahlman, and H. Levy II, On the origin of tropospheric ozone, *J. Geophys. Res.*, **85**, 7546-7552, 1980.

- Liu, S. C., M. McFarland, D. Kley, O. Zafiriou, and B. Huebert, Tropospheric NO<sub>x</sub> and O<sub>3</sub> budgets in the equatorial Pacific, *J. Geophys. Res.*, **88**, 1360-1368, 1983.
- Liu, S. C., M. Trainer, F. C. Fehsenfeld, D. D. Parrish, E. J. Williams, D. W. Fahey, G. Hübler, and P. C. Murphy, Ozone production in the rural troposphere and the implications for regional and global ozone distributions, *J. Geophys. Res.*, **92**, 4191-4207, 1987.
- Logan, J. A., Nitrogen oxides in the troposphere: Global and regional budgets, *J. Geophys. Res.*, **88**, 10,785-10,807, 1983.
- Logan, J. A., Tropospheric ozone: Seasonal behavior, trends, and anthropogenic influence, *J. Geophys. Res.*, **90**, 10,463-10,482, 1985.
- Logan, J. A., M. J. Prather, S. C. Wofsy, and M. B. McElroy, Tropospheric chemistry: A global perspective, *J. Geophys. Res.*, **86**, 7210-7254, 1981.
- Olszyna, K. J., E. M. Bailey, R. Simonaitis, and J. F. Meagher, O<sub>3</sub> and NO<sub>y</sub> relationships at a rural site, *J. Geophys. Res.*, **99**, 14,557-14,563, 1994.
- Parrish, D. D., M. Trainer, M. P. Buhr, B.A. Watkins, and F. C. Fehsenfeld, Carbon monoxide concentrations and their relation to concentrations of total reactive oxidized nitrogen at two rural U.S. sites, *J. Geophys. Res.*, **96**, 9309-9320, 1991.
- Parrish, D.D., J. S. Holloway, M. Trainer, P. C. Murphy, G. Forbes, and F. C. Fehsenfeld, Export of North American ozone to the North Atlantic Ocean, *Science*, **259**, 1436-1439, 1993a.
- Parrish, D.D., et al., The total reactive oxidized nitrogen levels and the partitioning between the individual species at six rural sites in eastern North America, *J. Geophys. Res.*, **98**, 2927-2939, 1993b.
- Ridley, B. A., Recent measurements of oxidized nitrogen compounds in the troposphere, *Atmos. Environ.*, **25A**, 1905-1926, 1991.
- Ridley, B. A., M. A. Carroll, and G. L. Gregory, Measurements of nitric oxide in the boundary layer and free troposphere over the Pacific Ocean, *J. Geophys. Res.*, **92**, 2025-2047, 1987.
- Ridley, B. A., M. A. Carroll, G. L. Gregory, and G. W. Sachse, Techniques and measurements in regions of a folded tropopause, *J. Geophys. Res.*, **93**, 15,813-15,830, 1988.
- Ridley, B. A., M. A. Carroll, D. D. Dunlap, M. Trainer, G. W. Sachse, G. L. Gregory, and E. P. Condon, Measurements of NO<sub>x</sub> over the eastern Pacific Ocean and southwestern United States during the spring 1984 NASA GTE aircraft program, *J. Geophys. Res.*, **94**, 5043-5067, 1989.
- Roberts, J.M., et al., Episodic removal of NO<sub>y</sub> species from the marine boundary layer over the North Atlantic, *J. Geophys. Res.*, this issue.
- Sandholm, S. T., J. D. Bradshaw, G. Chen, H. B. Singh, R. W. Talbot, G. L. Gregory, D. R. Blake, G. W. Sachse, E. V. Browell, J. W. Barrick, M. A. Shipham, A. S. Bachmeier, and D. Owen, Summertime tropospheric observations related to N<sub>x</sub>O<sub>y</sub> distributions and partitioning over Alaska: Arctic Boundary Layer Expedition 3A, *J. Geophys. Res.*, **97**, 16,481-16,510, 1992.
- Sandholm, S. T., et al., Summertime partitioning and budget of NO<sub>y</sub> compounds in the troposphere over Alaska and Canada: ABLE 3B, *J. Geophys. Res.*, **99**, 999-1964, 1994.
- Sandroni, S., D. Anfossi, and S. Viarango, Surface ozone levels at the end of the nineteenth century in South America, *J. Geophys. Res.*, **97**, 2535-2539, 1992.
- Trainer, M., et al., Correlation of ozone with NO<sub>y</sub> in photochemically aged air, *J. Geophys. Res.*, **98**, 2917-2925, 1993.
- Volz, A., and D. Kley, Evaluation of the Montsouris series of ozone measurements made in the nineteenth century, *Nature*, **332**, 240-242, 1988.
- 
- G. M. Albercook, M. A. Carroll, K. A. Duderstadt, A. N. Markevitch, and K. R. Owens, Department of Atmospheric, Oceanic, and Space Sciences, University of Michigan, Ann Arbor, MI 48109-2143. (e-mail: george\_ablercook@emal.sprl.umich.edu; mcarroll@umich.edu; kathyd@engin.umich.edu; aleksei@sassarch.sprl.umich.edu; krotech@metronet.com)
- F. C. Fehsenfeld, J. S. Holloway, and D. D. Parrish, Aeronomy Laboratory, National Oceanic and Atmospheric Administration, Boulder, CO 80303. (e-mail: fcf@al.noaa.gov; jholloway@al.noaa.gov; parrish@al.noaa.gov)
- G. Forbes, Atmospheric Environment Service, Sable Island, Nova Scotia, Canada. (e-mail: gforbes@fox.nstn.ca)
- J. Ogren, Climate Monitoring and Diagnostics Laboratory, National Oceanic and Atmospheric Administration, Boulder, CO 80303. (e-mail: johno@cmdl.noaa.gov)
- T. Wang, (corresponding author), Environmental Engineering Unit, Department of Civil and Structural Engineering, Hong Kong Polytechnic University, Hung Hom, Kowloon, Hong Kong. (e-mail: cetwang@polyu.edu.hk)

(Received May 4, 1995; revised March 11, 1996; accepted March 11, 1996.)